Hindawi Publishing Corporation
International Journal of Photoenergy
Volume 2015, Article ID 382814, 9 pages
http://dx.doi.org/10.1155/2015/382814

Research Article

Optimization of μc-$Si_{1-x}Ge_x$:H Single-Junction Solar Cells with Enhanced Spectral Response and Improved Film Quality

Yen-Tang Huang, Pei-Ling Chen, Po-Wei Chen, Hung-Jung Hsu, Cheng-Hang Hsu, and Chuang-Chuang Tsai

Department of Photonics, National Chiao Tung University, 1001 University Road, Hsinchu 300, Taiwan

Correspondence should be addressed to Yen-Tang Huang; yen.tang.huang@gmail.com

Received 3 April 2015; Accepted 15 June 2015

Academic Editor: Jürgen Hüpkes

Effects of RF power on optical, electrical, and structural properties of μc-$Si_{1-x}Ge_x$:H films was reported. Raman and FTIR spectra from μc-$Si_{1-x}Ge_x$:H films reflected the variation in microstructure and bonding configuration. Unlike increasing the germane concentration for Ge incorporation, low RF power enhanced Ge incorporation efficiency in μc-$Si_{1-x}Ge_x$:H alloy. By decreasing RF power from 100 to 50 W at a fixed reactant gas ratio, the optical bandgap of μc-$Si_{1-x}Ge_x$:H was reduced owing to the increase in Ge content from 11.2 to 23.8 at.%, while Ge-related defects and amorphous phase were increased. Consequently, photo conductivity of 1.62×10^{-5} S/cm was obtained for the μc-$Si_{1-x}Ge_x$:H film deposited at 60 W. By applying 0.9 μm thick μc-$Si_{1-x}Ge_x$:H absorber with X_C of 48% and [Ge] of 16.4 at.% in the single-junction cell, efficiency of 6.18% was obtained. The long-wavelength response of μc-$Si_{1-x}Ge_x$:H cell was significantly enhanced compared with the μc-Si:H cell. In the case of tandem cells, 0.24 μm a-Si:H/0.9 μm μc-$Si_{1-x}Ge_x$:H tandem cell exhibited a comparable spectral response as 0.24 μm a-Si:H/1.4 μm μc-Si:H tandem cell and achieved an efficiency of 9.44%.

1. Introduction

Thin-film silicon solar cells have the advantages of low material/energy consumption and the ability of large-area fabrication, which is beneficial for the long term production of photovoltaics. To stay competitive with other technologies, further improvement in conversion efficiency is important. By employing different bandgap absorbers that enable broad-band absorption of solar spectrum, the multijunction solar cells have been demonstrated as a viable approach to achieving high-efficiency devices. Taking advantages of ideal combination of absorber bandgaps [1], the hydrogenated amorphous silicon (a-Si:H)/hydrogenated microcrystalline silicon (μc-Si:H) tandem solar cells with stabilized cell efficiencies of over 10% have been demonstrated by many groups [2, 3]. However, due to the indirect bandgap of μc-Si:H material, absorber with few μm in thickness is needed for achieving sufficient light absorption in the bottom cell. To further enhance the optical absorption in the long-wavelength region, alloying germanium into μc-Si:H network has been purposed [4, 5].

The bandgap of hydrogenated microcrystalline silicon germanium (μc-$Si_{1-x}Ge_x$:H) can be narrowed from 1.12 eV toward 0.67 eV, depending on the Ge content (x) in the alloy [5–8]. Furthermore, Matsui et al. [5] have reported that μc-$Si_{0.5}Ge_{0.5}$:H had a high absorption coefficient of 10^4 cm^{-1} at 1.5 eV, which is approximately one order of magnitude higher than that of μc-Si:H. The thinner $Si_{1-x}Ge_x$:H cells have been employed to obtain a comparable photocurrent to μc-Si:H cells [9, 10]. Nevertheless, μc-$Si_{1-x}Ge_x$:H alloy is a complicated atomic network consisting of a mixed amorphous-crystalline phase and a Si-Ge-H multielement system. As a result, crystallization and Ge incorporation are bound up with the optical and electric properties for μc-$Si_{1-x}Ge_x$:H films. A sufficient crystalline phase is needed for the efficient carrier transport; however, the Ge incorporation in a microcrystalline Si network suppresses the crystallization in the growth of μc-$Si_{1-x}Ge_x$:H film [11]. The optimization

of crystalline volume fraction (X_C) and Ge content ([Ge]) by using the proper process parameters is important in the development of μc-$Si_{1-x}Ge_x$:H alloy.

Previous studies on μc-$Si_{1-x}Ge_x$:H alloy have demonstrated the correlation between germane concentration (R_{GeH_4}) and Ge incorporation [5, 9, 10, 12–14]. However, the impact of RF power on μc-$Si_{1-x}Ge_x$:H film properties has not yet been fully investigated. In this work, the effect of RF power on the optical, electrical, and microstructural properties of μc-$Si_{1-x}Ge_x$:H films has been presented and discussed in detail. Application of corresponding μc-$Si_{1-x}Ge_x$:H absorbers in single-junction cells and a-Si:H/μc-$Si_{1-x}Ge_x$:H tandem cells has also been performed and presented.

2. Experimental Detail

A 27.12 MHz plasma-enhanced chemical vapor deposition (PECVD) system, having a load-lock and a transfer chamber, was employed for the deposition of doped and undoped silicon based thin films. The process chamber was equipped with a 26×26 cm^2 plasma reactor. The interelectrode distance was 8 mm. In order to reduce cross contamination, the NF_3 in situ plasma cleaning was introduced in the single-chamber process. The μc-$Si_{1-x}Ge_x$:H films were deposited by a highly H_2-diluted gas mixture of silane (SiH_4) and germane (GeH_4). The hydrogen dilution ratio (R_{H_2}, defined as $[H_2]/[GeH_4+SiH_4]$) and the germane concentration (R_{GeH4}, defined as $[GeH_4]/[GeH_4+SiH_4]$) were kept at 94.9 and 5.06%, respectively. The RF power was varied in the range of 40–100 W with a pressure of 1000 Pa.

For the characterization of film properties, the 200 nm thick μc-$Si_{1-x}Ge_x$:H films were prepared on Corning EAGLE XG glass substrates at approximately 200°C. Besides, p-type Si (100) single side polished wafer was utilized as substrate for FTIR measurement. It is known that the crystalline volume fraction (X_C) had variation in the initial growth of microcrystalline materials. In this study, the noncrystallized region occupied only a small part of the films deposited on c-Si and glass substrates. The data obtained from different substrates should be self-consistent in this paper. In addition, FTIR data should be representative for the film and correspond to the cell performance for the 0.9 μm thick μc-$Si_{1-x}Ge_x$:H solar cells. For the quantitative estimation for X_C, the Raman equipment equipped with a diode-pumped solid-state laser and provided an excited wavelength of 488 nm. By using deconvolution of the Raman spectra, the peaks at 520 cm^{-1}, 494–507 cm^{-1}, and 480 cm^{-1} correspond to crystalline, intermediate, and amorphous phases, respectively [15–17]. In addition, the Ge-related peaks [18, 19] centered at 400, 370, 300, and 270 cm^{-1} were attributed to the signals of c-Si-Ge, a-Si-Ge, c-Ge-Ge, and a-Ge-Ge, respectively.

For determining a quantitative composition in the μc-$Si_{1-x}Ge_x$:H film, an X-ray photoelectron spectroscopy (XPS) was used to measure the intensities of Ge*3d* and Si*2p* core lines for the estimation of the film Ge content [20]. The hydride bonding configuration was characterized by FTIR spectra. A UV-VIS-NIR spectroscopy was used to measure the transmittance (T) and the reflectance (R) to obtain the absorption coefficient (α). By using T and R, the intercept

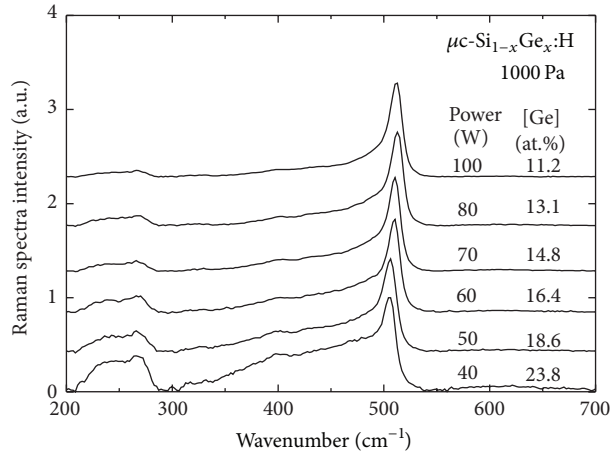

Figure 1: Raman spectra for the μc-$Si_{1-x}Ge_x$:H films deposited with the different RF powers.

of Tauc's plot of $(\alpha h\nu)^{1/2}$ versus $h\nu$ (photon energy) is commonly used to evaluate Tauc gap. However, the μc-Si phase segregation in alloys [21] and the mixed phase [22] in microcrystalline materials would produce interference fringe. As an alternative indication for an optical property of μc-$Si_{1-x}Ge_x$:H film, the optical bandgap (E_{04}) was used in the study, which was determined by the energy of the photon at the absorption coefficient of 10^4 cm^{-1}.

Finally, the 0.9 μm thick μc-$Si_{1-x}Ge_x$:H single-junction cells and a-Si:H/μc-$Si_{1-x}Ge_x$:H tandem solar cells with a thickness of 0.24/0.9 μm were prepared on the commercial textured SnO_2:F-coated glass in a superstrate (p-i-n) configuration. The cell with a device area of 0.25 cm^2 was characterized by an AM1.5G solar simulator and a current-voltage measurement. An external quantum efficiency (EQE) measurement was implemented under both short-circuit and reverse voltage-biased conditions to reveal the behaviors of carrier transport and spectral response in the solar cells.

3. Results and Discussion

3.1. Effect of RF Power on the Properties of μc-$Si_{1-x}Ge_x$:H Films. Figure 1 shows the Raman spectra of μc-$Si_{1-x}Ge_x$:H alloy prepared at the different RF power. With a decreasing RF power from 100 to 40 W, more amorphous Si phase was deposited, accompanied with less crystalline phase. In addition, the [Ge] was increased from 11.2 to 23.8 at.%, with the c-Si-Si peak shifted from 513 to 504 cm^{-1}. The red-shift of c-Si-Si peak with the increase in Ge content has also been reported in the previous works [4, 23]. This is likely owing to the compressive strain induced by the Ge bond at the neighborhood of c-Si network [17]. Moreover, as the RF power reduced from 100 to 40 W, the intensity of Ge-related peaks at 400, 370, and 270 cm^{-1} increased, which coincided with the increase in Ge content. The substantial increase in a-Ge-Ge and a-Si-Ge peaks indicated a fraction of Ge was incorporated into amorphous phase and thus suppressed the formation of crystalline phase.

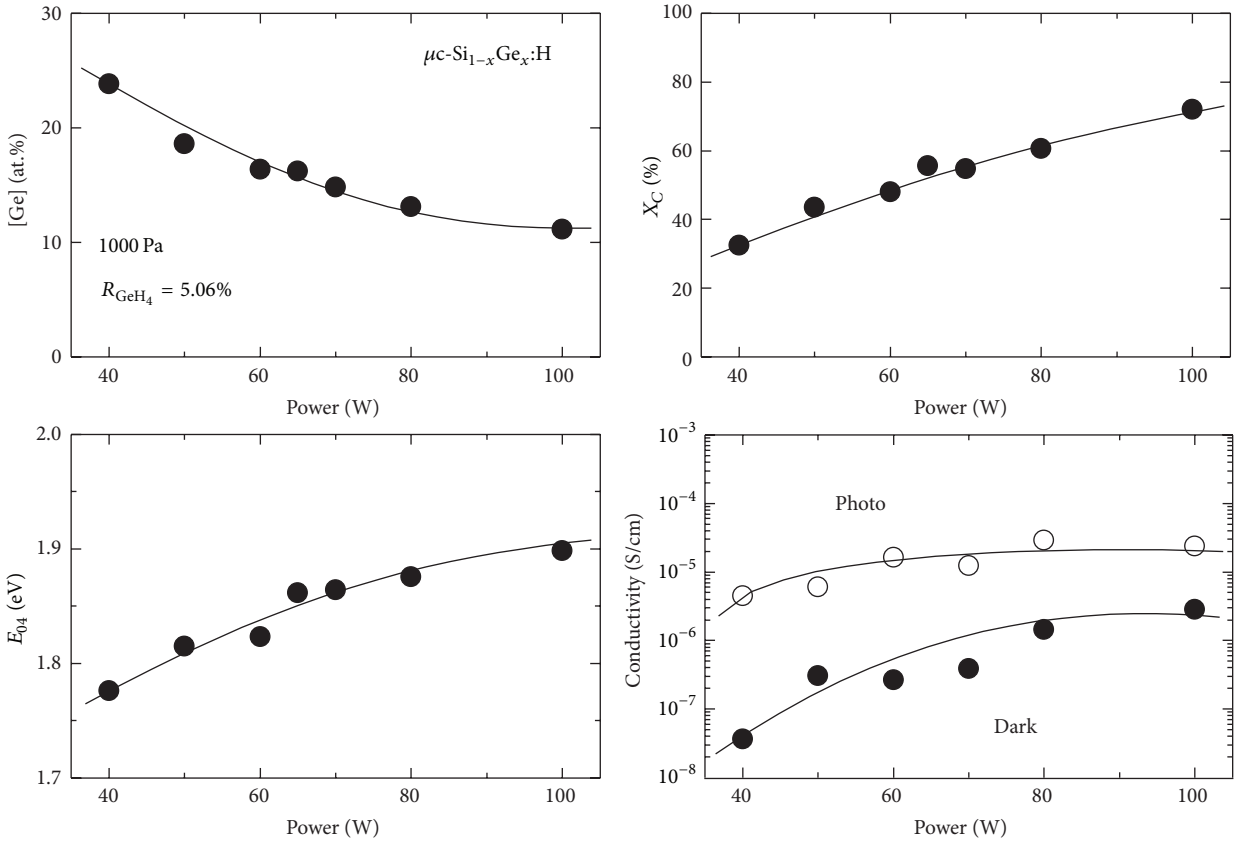

Figure 2: Dependence of μc-$Si_{1-x}Ge_x$:H film properties, [Ge], X_C, E_{04}, and conductivity, on reaction RF power. For the conductivity, the open and closed circle symbols, respectively, represent photo- and dark conductivities.

Moreover, the weak peak at approximately 247 cm^{-1} was observed in μc-$Si_{1-x}Ge_x$:H alloys, which was originated from the resonant mode [23, 24] and overlapped with amorphous background of Ge–Ge mode. Another weak peak at 430 cm^{-1} was assigned to a localized Si–Ge phonon mode. Furthermore, in our case, the c-Ge-Ge peak at 300 cm^{-1} was not found, which may be due to the low Ge content in μc-$Si_{1-x}Ge_x$:H films ([Ge] < 25 at.%). The studies of Raman spectra in $Si_{1-x}Ge_x$ alloys have suggested that the c-Ge-Ge peak was broadened and the intensity rapidly decreased as Ge content was lower than 50 at.% [19, 23].

Although most peaks can be deconvoluted, the precise estimation for crystalline volume fraction of μc-$Si_{1-x}Ge_x$:H films is not easy to be determined. With less Ge content ([Ge] < 25 at.%) in μc-$Si_{1-x}Ge_x$:H alloys, the Ge-related modes having broadened shoulder were difficult to be separated. In this study, weak integrated intensity of c-Ge-Ge mode was ignored in the contribution of crystalline column fraction. To obtain a quantified value to compare the degree of crystallization, the X_C was calculated by the ratio of $(I_c + I_m)/(I_c+I_m+I_a)$, where the integrated intensities of crystalline (I_c), intermediate (I_m), and amorphous (I_a) Si phases in Raman spectra were used [16, 25].

Figure 2 demonstrates the effects of RF power on [Ge], X_C, E_{04}, and the conductivity of μc-$Si_{1-x}Ge_x$:H films. As the RF power decreased from 100 to 40 W, the [Ge] significantly increased from 11.2 to 23.8 at.%. In the plasma of PECVD process, the generation of growth precursor is proportional to the density of energetic electrons which are responsible for the reaction and the dissociation cross section [26]. The dissociation energies are 83.4 and 91.7 kcal/mole for GeH_4 and SiH_4, respectively [27]. Lower power reduces the energy of electron in the plasma and thus shifts the dissociation thresholds for SiH_4 and GeH_4. As a result, relatively more Ge-related precursors were in the gas phase which leads to more Ge incorporation in the solid phase [28]. Moreover, the Ge incorporation efficiency ($[Ge]/R_{GeH_4}$) indicates the capability of Ge atom transfer from gas phase into solid state. In the case of all samples, the $[Ge]/R_{GeH_4}$ was larger than one, suggesting that Ge was preferentially incorporated in μc-$Si_{1-x}Ge_x$:H films compared to Si. As the RF power decreased from 100 to 40 W, the $[Ge]/R_{GeH_4}$ was enhanced from 2.2 to 4.7. This indicated that the lower RF power significantly promoted Ge incorporation for μc-$Si_{1-x}Ge_x$:H growth.

In comparison to the effect of RF power, the film Ge content in μc-$Si_{1-x}Ge_x$:H alloy can also be increased by directly increasing GeH_4 concentration. According to the research results of Matsui et al. and our previous work, the nonlinear behavior of Ge incorporation was observed and reflected a decrease in Ge incorporation efficiency by adding GeH_4 in SiH_4-GeH_4-H_2 plasma [10, 11]. More sticky GeH_3 growth precursors would be produced and increased the

weak Ge-related bonds on the growth surface [29, 30]. In the hydrogen-containing plasma atmosphere, the probability of SiH_3 precursors replacing the weak Ge-bonded site may be enhanced. Thus the drop in Ge incorporation efficiency was found when the R_{GeH_4} was increased.

Matsui et al. [10, 31] have also reported that the Ge content of μc-$Si_{1-x}Ge_x$:H films prepared in 100 MHz VHF-PECVD with 130 cm^2 reactor was slightly changed by only 2% in the power density range from 0.12 to 0.23 W/cm^2. At a higher RF frequency and a relatively higher power density, the GeH_4 and SiH_4 may be completed dissociated in the plasma. In contrast, a lower RF frequency of 27.12 MHz and a lower power density ranging from 0.06 to 0.15 W/cm^2 for μc-$Si_{1-x}Ge_x$:H preparation were used in this research.

As illustrated in Figure 2, accompanied with the increase in Ge content as RF power decreased from 100 to 40 W, the optical bandgap (E_{04}) decreased from 1.90 to 1.78 eV. The bandgap at temperature of 298 K for pure Si and Ge films was 1.12 and 0.67 eV [6, 8]. Since the Ge atoms incorporated into the Si-Si network, the bandgap structure would be changed by Ge atoms. With a smaller bandgap of Ge, alloying Ge in Si-Si network could shift the bandgap toward Ge network. At a lower power, the enhanced Ge incorporation in the μc-$Si_{1-x}Ge_x$:H films contributed to bandgap narrowing, which led to a significant drop by 0.12 eV in the optical bandgap.

Furthermore, with a decreased RF power from 100 to 40 W, the X_C decreased from 72.1% to 32.5%, as shown in Figure 1. Kondo et al. [32] reported that a moderate increase in RF power depleted SiH_4 and facilitated the crystallization. In addition, a properly high power density for a-$Si_{1-x}Ge_x$:H growth improved film quality [28]. Increasing RF power transferred more momentum and energy to precursors, especially for the sticky Ge-related precursors. The longer diffusion length of the precursors promotes network relaxation in SiGe matrix. Therefore, more amorphous phase in μc-$Si_{1-x}Ge_x$:H films was observed at a lower RF power.

As demonstrated in Figure 2, when the RF power decreased from 100 to 60 W, the photoconductivity was kept at approximately 2.0×10^{-5} S/cm. With the decreasing dark conductivity, the increased photo-to-dark conductivity ratio from 8 to 60 was found. The bandgap narrowing resulting from Ge incorporation can contribute to more optical absorption and more photon-generated carriers. On the other hand, Vetterl et al. [33] reported that the light absorption coefficient of a-Si:H films is significantly less than that of μc-Si:H films in the photon energies below 1.7 eV. For structural transition from crystalline to amorphous phase, more amorphous phase in μc-$Si_{1-x}Ge_x$:H films would lower the contribution of light absorption in the long-wavelength region. In addition, the relatively low mobility and lifetime for carriers are expected in a-Si:H film. The Ge incorporation and microstructural evolution are in competition. As a result, no significant change in the photoconductivity was observed. As RF power was less than 60 W, the photoconductivity rapidly decreased to less than 6.1×10^{-6} S/cm. Too much amorphous phase in the μc-$Si_{1-x}Ge_x$:H films, having an X_C less than 48%, degraded the contribution in the photocurrent. Moreover, the more Ge-induced defects also could degrade the carrier transport. On the other hand, when RF power decreased from 100 to 40 W, the dark conductivity decreased from 2.9×10^{-6} to 8.5×10^{-8} S/cm. As amorphous phase increased, the activation energy increased due to fewer defects, which originated from grain boundary [15]. The thermal excitation through gap states decreased and led to a lower dark conductivity.

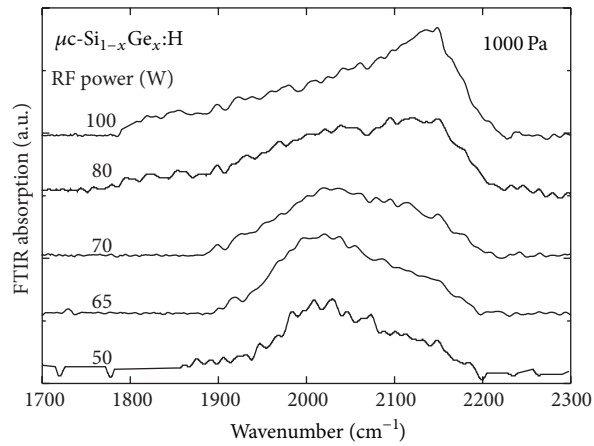

FIGURE 3: FTIR spectra for the μc-$Si_{1-x}Ge_x$:H films deposited with the different RF powers.

Figure 3 shows FTIR spectra of the μc-$Si_{1-x}Ge_x$:H films deposited at different RF power. In the case of μc-$Si_{1-x}Ge_x$:H film prepared at 100 W, relatively high IR absorption from 2080 to 2150 cm^{-1} was observed. In this region, three narrow high stretching modes (NHSMs) at 2083, 2102, and 2137 cm^{-1} which correspond to SiH, SiH_2, and SiH_3 at crystalline grain boundaries, respectively [34], were reported as a signature of porous and less-dense structure in high-X_C μc-Si:H network [35]. The presence of NHSMs in our case increased the carrier recombination loss and thus reduced the electrical property (Figure 2). Another two high SMs (HSMs) at 2120 and 2150 cm^{-1} were ascribed to SiH_2 and SiH_3 which resulted from the macroscopic amorphous surfaces in μc-Si:H films. As the power was reduced from 100 to 50 W, both NHSMs and HSMs were reduced due to the reduction in X_C. The reduced NHSMs indicated that the micro voids or vacancies at the grain boundary were reduced, leading to a more compact structure [35]. This coincided with the decrease in dark conductivity as the power decreased from 100 to 50 W. In addition, the SMs ranging in 1980–2010 cm^{-1} and 2070–2100 cm^{-1} were SiH and SiH_2 bonding, which reflected silicon hydrides in the bulk amorphous phase [36].

In the case of μc-$Si_{1-x}Ge_x$:H films prepared at 80 and 100 W, the presence of component at 1880 cm^{-1} reflected the mode of GeH [28, 37]. As RF power was less than 80 W, the GeH bonding was absent. This result suggested that sufficient power is beneficial in providing energy for structure relaxation of Ge-related precursors [38]. A lower RF power for μc-$Si_{1-x}Ge_x$:H growth provided less energy to the precursors and shortened the diffusion lengths for the precursors, especially in sticky Ge-related precursors. The Ge-related precursors easily stuck on the growth surface without seeking a minimum energy bond site and formed the Ge-related

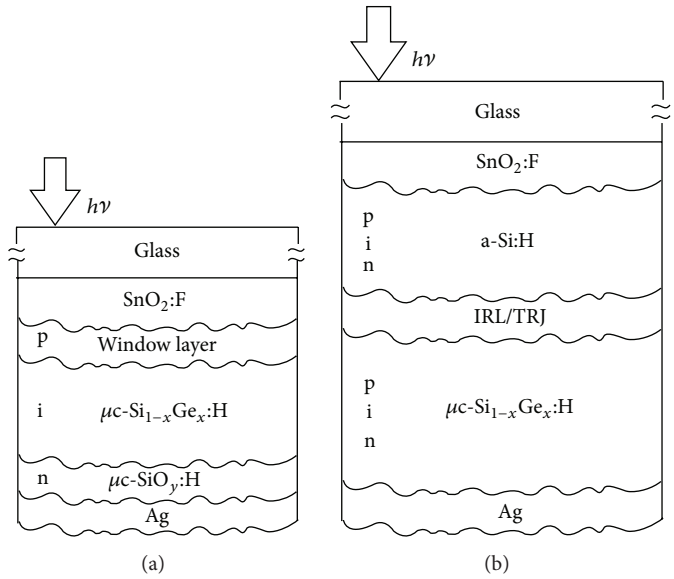

FIGURE 4: Cross section of μc-$Si_{1-x}Ge_x$:H p-i-n single-junction and a-Si:H/μc-$Si_{1-x}Ge_x$:H tandem cells.

weak bonds. According to the XPS result, the increase in Ge incorporation contributed to SiGe network, which narrowed the bandgap. The enhanced light absorption promoted more photo-generated carriers. Nevertheless, the carriers transport was probably recombined by the increase in Ge-induced defects. Ge incorporation could easily induce interconnected microvoids and dangling bonds. This increased the heterogeneity in the SiGe matrix and provided recombination centers for charged carriers, which was different from the midgap defects [28]. Furthermore, previous works showed that Ge incorporation induced an acceptor-like state at the grain boundary in μc-$Si_{1-x}Ge_x$:H [5, 31]. This acceptor-like state weakened the electric field near p/i interface in μc-$Si_{1-x}Ge_x$:H p-i-n solar cells. Being considered by the effects of Ge incorporation on light absorption and formation of Ge-related defect, the photo-to-dark conductivity gain could be found to be 60 in an optimized μc-$Si_{1-x}Ge_x$:H absorbing film. These corresponded to the μc-$Si_{1-x}Ge_x$:H film prepared at 60 W with pretty good photoconductivity of 1.62×10^{-5} S/cm.

3.2. Application of μc-$Si_{1-x}Ge_x$:H Absorber in Single-Junction Solar Cells and a-Si:H/μc-$Si_{1-x}Ge_x$:H Tandem Cells. In this section, the application of μc-$Si_{1-x}Ge_x$:H absorber in device and the cell performance were presented and discussed. Figure 4 demonstrates the schematic cross section of μc-$Si_{1-x}Ge_x$:H single-junction solar cells and a-Si:H/μc-$Si_{1-x}Ge_x$:H tandem cells with 0.9 μm thick μc-$Si_{1-x}Ge_x$:H absorber.

Figure 5(a) demonstrates the EQE of μc-$Si_{1-x}Ge_x$:H single-junction cells with absorber prepared at different RF power. With the decreasing of RF power from 100 to 50 W, the EQE was slightly enhanced at wavelengths from 550 to 720 nm. This can be ascribed to the increased Ge content from 11.2 to 23.8 at.%, which narrowed the bandgap and led to the enhanced light absorption in long-wavelength region. On the other hand, as the power decreased from 100 to 50 W, there was a reduction in the blue response (< 700 nm). Since the X_C was reduced at a lower RF power, the μc-$Si_{1-x}Ge_x$:H absorber near the p-layer could be defective owing to more amorphous phase. At the first few tens of nanometers of the film, more amorphous phase led to a barrier that reduced carrier mobility. This increased the recombination loss and resulted in carrier extraction problems at the p/i interface [39].

To clarify the carrier collection in the μc-$Si_{1-x}Ge_x$:H cell, the reverse-bias EQE was measured. Figure 5(b) compares the EQEs of μc-$Si_{1-x}Ge_x$:H cell with bias voltage of 0 and −1 V. The cell with μc-$Si_{1-x}Ge_x$:H absorber prepared at 50 W was used. When the reverse bias was applied, EQE was enhanced at the wavelength from 350 to 750 nm with an increased current density by 0.89 mA/cm^2. This suggested that carriers trapped in the bulk absorber due to the presence of Ge-induced defects were driven out and were collected. In contrast to the cell with μc-$Si_{1-x}Ge_x$:H absorber prepared at 50 W, cells with μc-$Si_{1-x}Ge_x$:H absorber prepared from 60 to 100 W exhibited additional increase in current density by less than 0.4 mA/cm^2 under reverse-bias condition. This suggested that the carrier collection across the p/i region can be improved by reducing Ge-induced defects and amorphous phase.

As compared with the single-junction cell having 0.9 μm thick μc-Si:H absorber, the μc-$Si_{1-x}Ge_x$:H cells exhibited a substantial enhancement in EQE at the wavelength from 500 to 1100 nm (Figure 5(b)). The J_{SC} was increased by 2.8 mA/cm^2. This shows that the μc-$Si_{1-x}Ge_x$:H single-junction solar cells had more superior spectral response than μc-Si:H single-junction solar cells, especially in the red-to-infrared region, which was beneficial in the multijunction configuration.

The performance of μc-$Si_{1-x}Ge_x$:H single-junction cells with μc-$Si_{1-x}Ge_x$:H absorbers deposited at different RF power is illustrated in Figure 6. The performance of the μc-Si:H cell

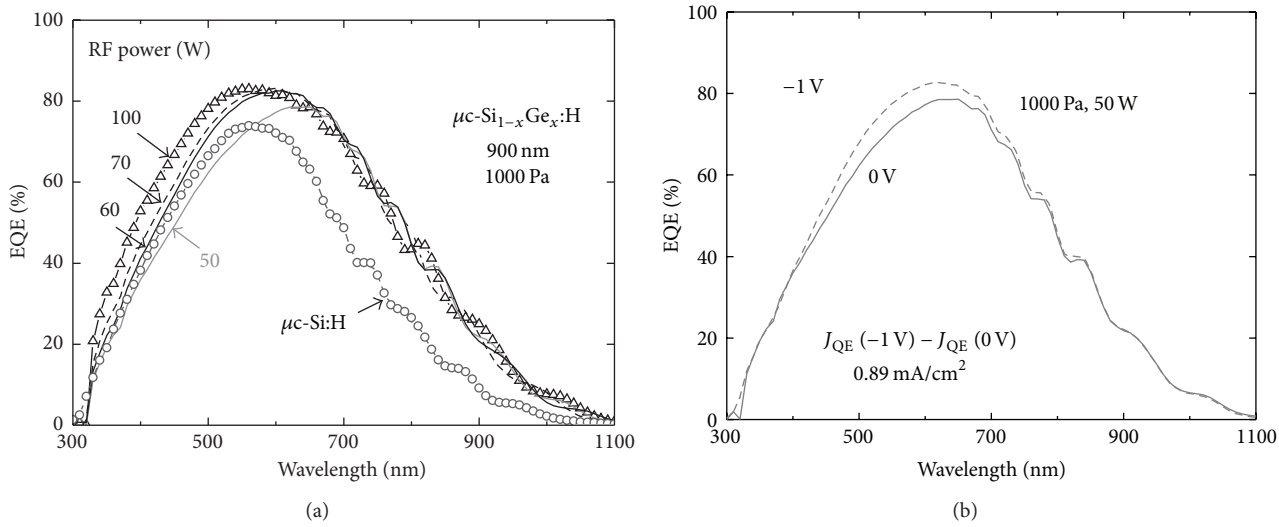

FIGURE 5: (a) EQE of single-junction cells using μc-$Si_{1-x}Ge_x$:H absorbers deposited at different RF power of 100 W (line with open triangle), 70 W (dash line), 60 W (solid line), and 50 W (grey line). The EQE for μc-Si:H cell was represented by the line with open circle. (b) The EQE with −1 V bias and 0 V for the cell using the μc-$Si_{1-x}Ge_x$:H absorber deposited at 50 W.

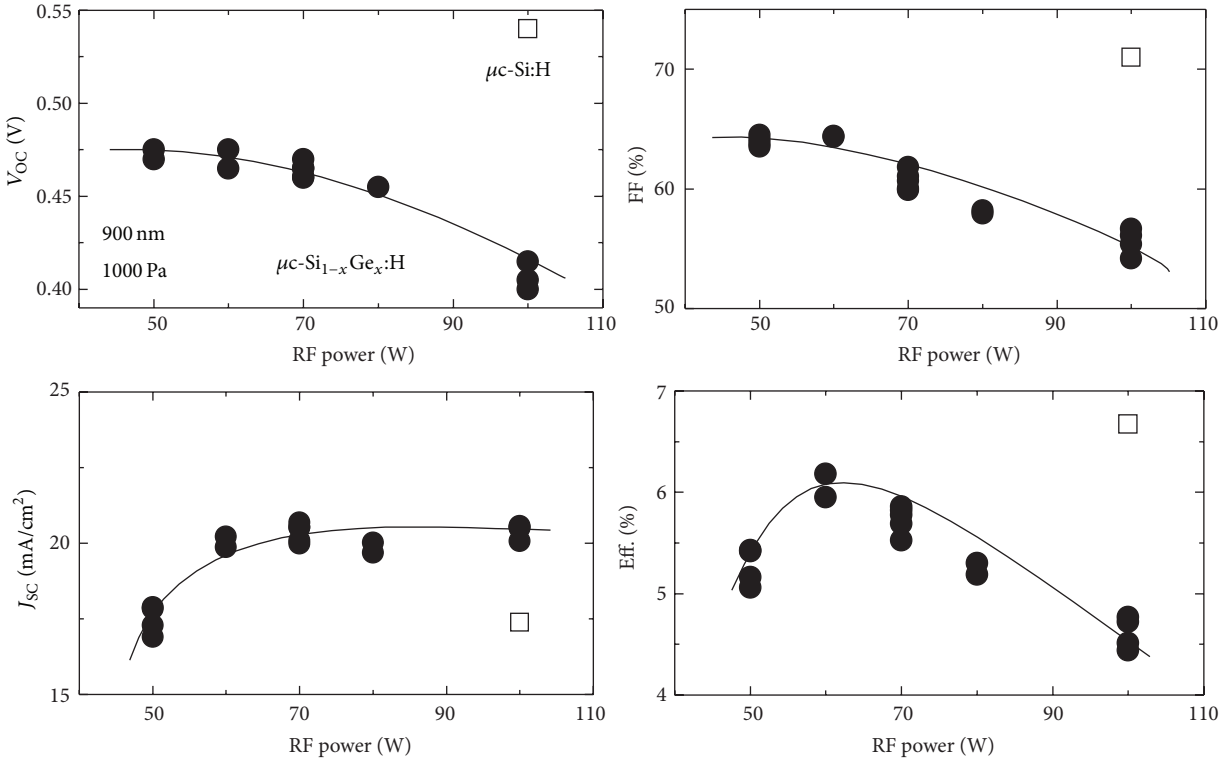

FIGURE 6: Performance of μc-$Si_{1-x}Ge_x$:H single-junction cells with absorbers deposited under different RF powers. The performance of μc-Si:H cell is represented by the open square.

with 0.9 μm thick absorber (X_C ~50%) was also shown for comparison. As can be seen from Figure 6, the short-circuit current density (J_{SC}) was kept approximately 20 mA/cm^2 as the power decreased from 100 to 60 W. This was due to the enhancement in the long-wavelength response accompanied with the reduction in short-wavelength response. When the RF power was further decreased to 50 W, the J_{SC} was reduced to 17.3 mA/cm^2 with the corresponding [Ge] increasing to 18.6 at.%. The reduction in J_{SC} can be attributed to the increase in Ge-related defects which worsened the carrier

Table 1: Comparison of cell performance for tandem solar cells, having the 0.24 μm thick a-Si:H top cell stacked with different bottom absorbers.

Bottom absorber	V_{OC} (V)	J_{SC} (mA/cm^2)	FF (%)	Eff. (%)	J_{QE} (mA/cm^2)		
					Top	Bot.	Total
0.9 μm μc-Si$_{1-x}$Ge$_x$:H	1.33	10.18	69.7	9.44	11.28	11.39	22.67
1.4 μm μc-Si:H	1.34	10.39	72.0	10.07	11.27	11.00	22.27

transport in the μc-Si$_{1-x}$Ge$_x$:H absorber. This can also be supported by the reduced photoconductivity as power reduced to 50 W.

On the other hand, the enhancement of the fill factor (FF) from 56.1% to 64.3% was found when the RF power decreased from 100 to 60 W. This was likely due to the reduction in voids and vacancies at the grain boundary in μc-Si$_{1-x}$Ge$_x$:H absorber as suggested by the decreased NHSMs (Figure 3). The voids and vacancies induced structural defects where the carrier would be recombined. Similar effect of NHSMs on the performance of μc-Si:H cells has also been reported [35, 40]. In addition, as the RF power decreased from 100 to 60 W, the open-circuit voltage (V_{OC}) of μc-Si$_{1-x}$Ge$_x$:H cells had a monotonic increase from 0.40 to 0.47 V (average value). This could be due to the suppression of defects at grain boundary, leading to the reduction in reverse saturation current. The reverse saturation current density of μc-Si$_{1-x}$Ge$_x$:H cells was decreased from 2.76×10^{-6} to 7.02×10^{-7} A/cm^2, indicating less leakage path and recombination loss of carriers in the cells. When the power was further reduced to 50 W, the V_{OC} and FF leveled off. This could be due to too much Ge-induced defects in the film, which hindered the carrier transport and degraded electrical property. With the μc-Si$_{1-x}$Ge$_x$:H absorber deposited at 60 W and 1000 Pa, the single-junction cell efficiency of 6.18% was obtained with V_{OC} = 0.475 V, FF = 64.3%, and J_{SC} = 20.22 mA/cm^2. The corresponding [Ge] and X_C of this μc-Si$_{1-x}$Ge$_x$:H film were 16.4 at.% and 48%, respectively.

Compared to the state-of-the-art μc-Si$_{1-x}$Ge$_x$:H single-junction solar cell [41] having an efficiency of 8.2% with J_{SC} = 25.5 mA/cm^2, V_{OC} = 0.494 V, and FF = 0.651, the comparable V_{OC}, FF, and lower J_{SC} were obtained in this research. The difference in front of TCO layer and antireflection coating [42] is likely to be the main reason for the lower J_{SC}. For the fabrication of microcrystalline silicon based single-junction solar cells, the front TCO plays an important role in the cell performance. Microcrystalline Si-based materials usually require the highly diluted H_2-containing plasma for an adequate X_C. Unfortunately, the commercial SnO_2:F-coated substrate is much chemically unstable than the ZnO:Ga in the hydrogen-rich plasma. Therefore, the a-Si:H(p)/μc-Si:H(p) bi-layer was used as the p-type window layer for protection of SnO_2:F surface for resisting Sn reduction, as reported in our previous work [43].

To demonstrate the improvement of using μc-Si$_{1-x}$Ge$_x$:H as the absorber of bottom cell, the a-Si:H/μc-Si$_{1-x}$Ge$_x$:H tandem cell was fabricated. The n-type μc-SiO$_y$:H with oxygen content of 8.5 at.%, optical gap (E_{04}) of 2.13 eV, and conductivity of 8×10^{-2} S/cm was employed as the

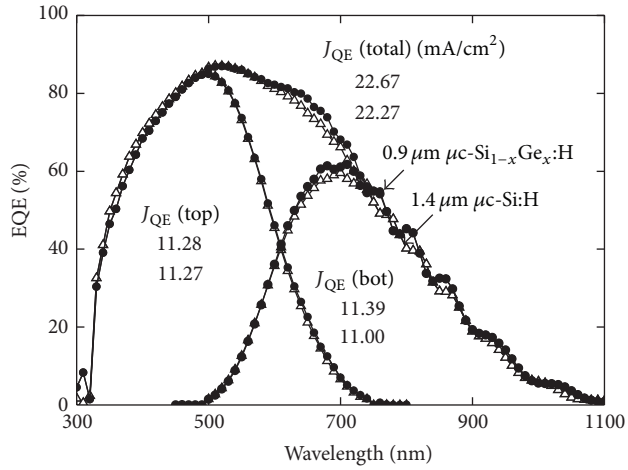

Figure 7: EQE of tandem cells in structures of a-Si:H top cells stacked with different bottom cells.

intermediate reflective layer (IRL) between the component cells. Detail on the study of IRL was reported in our previous work [44]. Table 1 summarizes the cell performance of a-Si:H (0.24 μm)/μc-Si$_{1-x}$Ge$_x$:H (0.9 μm) and a-Si:H (0.24 μm)/μc-Si:H (1.4 μm) tandem cells. In comparison with the cell having 1.4 μm thick μc-Si:H bottom absorber, the cell with the 0.9 μm thick μc-Si$_{1-x}$Ge$_x$:H bottom absorber exhibited a comparable V_{OC} of 1.33 V with a slightly lower FF of 69.7%. The latter can be ascribed to the Ge-induced defects which adversely influenced the carrier transport in μc-Si$_{1-x}$Ge$_x$:H cell. Notably, the tandem cell using 0.9 μm thick μc-Si$_{1-x}$Ge$_x$:H as bottom absorber exhibited comparable J_{SC} of 10.18 mA/cm^2 compared to the cell with 1.4 μm thick μc-Si:H absorber, which was confirmed by the quantum efficiency result shown in Figure 7. There was no significant difference of EQE in short-wavelength region, whereas a slight increase in spectral response was found at the wavelength from 600 to 1100 nm in the case of a-Si:H/μc-Si$_{1-x}$Ge$_x$:H tandem cell. Using a 0.9 μm thick μc-Si$_{1-x}$Ge$_x$:H bottom absorber in tandem cell exhibited the bottom cell J_{SC} of 11.39 mA/cm^2, which was 0.39 mA/cm^2 higher than that of the cell with 1.4 μm thick μc-Si:H bottom absorber. Compared with the μc-Si:H absorber, employment of μc-Si$_{1-x}$Ge$_x$:H reduced the absorber thickness by over 30%. The corresponding total current density can reach 22.67 mA/cm^2. The results indicated that a relative thin bottom absorber can be used for a sufficient IR absorption, fulfilled by applying the μc-Si$_{1-x}$Ge$_x$:H bottom absorber in Si-based tandem cells. The conversion efficiency for the 0.24 μm thick a-Si:H/0.9 μm

thick μc-$Si_{1-x}Ge_x$:H tandem cell was obtained as 9.44%, with J_{SC} = 10.18 mA/cm^2, V_{OC} = 1.33 V, and FF = 69.7%. The μc-$Si_{1-x}Ge_x$:H cell can be an important building block as the bottom cell in high-efficiency triple- or quadruple-junction cells that had the potential to obtain efficiency of 20% [45].

4. Conclusions

In this study, the effects of RF power on optical, electrical, and structural properties of μc-$Si_{1-x}Ge_x$:H films were investigated. Decreasing RF power density significantly increased Ge incorporation in μc-$Si_{1-x}Ge_x$:H films. The increased Ge content led to the bandgap narrowing. However, low-energy plasma weakened structural relaxation and the crystalline volume fraction decreased. FTIR data showed that the defective narrow high stretching modes (NHSMs) were found in μc-$Si_{1-x}Ge_x$:H deposited at high RF power. However, H passivation was less effective at a low RF power. Consequently, photoconductivity of 1.62×10^{-5} S/cm and a better film quality of μc-$Si_{1-x}Ge_x$:H was obtained at 60 W. The corresponding X_C and [Ge] were 48% and 16.4%, respectively. The cell efficiency for 0.9 μm thick μc-$Si_{1-x}Ge_x$:H single-junction cell achieved 6.18% with V_{OC} = 0.475 V, FF = 64.3%, and J_{SC} = 20.22 mA/cm^2. Compared to the μc-Si:H cell, the QE measurement showed that the long-wavelength response of μc-$Si_{1-x}Ge_x$:H cell was significantly enhanced. With a much thinner bottom absorber thickness, 0.24 μm a-Si:H/0.9 μm μc-$Si_{1-x}Ge_x$:H tandem cell exhibited a comparable spectral response as 0.24 μm a-Si:H/1.4 μm μc-Si:H tandem cell and achieved a cell efficiency of 9.44%.

Conflict of Interests

The authors do not have any conflict of interests with the content of the paper.

Acknowledgment

This work was sponsored by Ministry of Science and Technology in Taiwan under Grant no. 103-3113-P-008-001.

References

[1] M. A. Green, "Third generation photovoltaics: ultra-high conversion efficiency at low cost," *Progress in Photovoltaics: Research and Applications*, vol. 9, no. 2, pp. 123–135, 2001.

[2] J. Meier, S. Dubail, J. Cuperus et al., "Recent progress in micromorph solar cells," *Journal of Non-Crystalline Solids*, vol. 227–230, no. 2, pp. 1250–1256, 1998.

[3] B. Rech, O. Kluth, T. Repmann et al., "New materials and deposition techniques for highly efficient silicon thin film solar cells," *Solar Energy Materials and Solar Cells*, vol. 74, no. 1–4, pp. 439–447, 2002.

[4] G. Ganguly, T. Ikeda, T. Nishimiya, K. Saitoh, M. Kondo, and A. Matsuda, "Hydrogenated microcrystalline silicon germanium: a bottom cell material for amorphous silicon-based tandem solar cells," *Applied Physics Letters*, vol. 69, no. 27, Article ID 4224, 1996.

[5] T. Matsui, M. Kondo, K. Ogata, T. Ozawa, and M. Isomura, "Influence of alloy composition on carrier transport and solar cell properties of hydrogenated microcrystalline silicon-germanium thin films," *Applied Physics Letters*, vol. 89, Article ID 142115, 2006.

[6] J. Weber and M. I. Alonso, "Near-band-gap photoluminescence of Si-Ge alloys," *Physical Review B*, vol. 40, no. 8, pp. 5683–5693, 1989.

[7] R. Braunstein, A. R. Moore, and F. Herman, "Intrinsic optical absorption in germanium-silicon alloys," *Physical Review*, vol. 109, no. 3, pp. 695–710, 1958.

[8] A. Braun, A. Vossier, E. A. Katz, N. J. Ekins-Daukes, and J. M. Gordon, "Multiple-bandgap vertical-junction architectures for ultra-efficient concentrator solar cells," *Energy and Environmental Science*, vol. 5, no. 9, pp. 8523–8527, 2012.

[9] M. Isomura, K. Nakahata, M. Shima et al., "Microcrystalline silicon-germanium solar cells for multi-junction structures," *Solar Energy Materials and Solar Cells*, vol. 74, no. 1–4, pp. 519–524, 2002.

[10] T. Matsui, K. Ogata, M. Isomura, and M. Kondo, "Microcrystalline silicon-germanium alloys for solar cell application: growth and material properties," *Journal of Non-Crystalline Solids*, vol. 352, no. 9-20, pp. 1255–1258, 2006.

[11] Y. T. Huang, H. J. Hsu, S. W. Liang, C. H. Hsu, and C. C. Tsai, "Development of hydrogenated microcrystalline silicon-germanium alloys for improving long-wavelength absorption in Si-based thin-film solar cells," *International Journal of Photoenergy*, vol. 2014, Article ID 579176, 7 pages, 2014.

[12] C. W. Chang, T. Matsui, and M. Kondo, "Electron spin resonance study of hydrogenated microcrystalline silicon-germanium alloy thin films," *Journal of Non-Crystalline Solids*, vol. 354, no. 19–25, pp. 2365–2368, 2008.

[13] J. K. Rath, F. D. Tichelaar, and R. E. I. Schropp, "Heterogeneous growth of microcrystalline silicon germanium," *Solar Energy Materials and Solar Cells*, vol. 74, no. 1–4, pp. 553–560, 2002.

[14] S. Miyazaki, H. Takahashi, H. Yamashita, M. Narasaki, and M. Hirose, "Growth and characterization of microcrystalline silicon-germanium films," *Journal of Non-Crystalline Solids*, vol. 299-302, no. 1, pp. 148–152, 2002.

[15] D. Han, G. Yue, J. D. Lorentzen, J. Lin, H. Habuchi, and Q. Wang, "Optical and electronic properties of microcrystalline silicon as a function of microcrystallinity," *Journal of Applied Physics*, vol. 87, no. 4, pp. 1882–1888, 2000.

[16] A. Fedala, C. Simon, N. Coulon, T. Mohammed-Brahim, M. Abdeslam, and A.-C. Chami, "Low temperature deposition of microcrystalline silicon germanium $Si_{1-x}Ge_x$ by RF-PECVD," *Physica Status Solidi C*, vol. 7, no. 3-4, pp. 762–765, 2010.

[17] M. Luysberg, P. Hapke, R. Carius, and F. Finger, "Structure and growth of hydrogenated microcrystalline silicon: investigation by transmission electron microscopy and Raman spectroscopy of films grown at different plasma excitation frequencies," *Philosophical Magazine A*, vol. 75, no. 1, pp. 31–47, 1997.

[18] P. D. Persans, A. F. Ruppert, B. Abeles, and T. Tiedje, "Raman scattering study of amorphous Si-Ge interfaces," *Physical Review B*, vol. 32, no. 8, pp. 5558–5560, 1985.

[19] S.-F. Ren, W. Cheng, and P. Y. Yu, "Microscopic investigation of phonon modes in SiGe alloy nanocrystals," *Physical Review B*, vol. 69, no. 23, Article ID 235327, 2004.

[20] M. P. Seah, "The quantitative analysis of surfaces by XPS: a review," *Surface and Interface Analysis*, vol. 2, no. 6, pp. 222–239, 1980.

[21] M. M. Giangregorio, M. Losurdo, A. Sacchetti, P. Capezzuto, and G. Bruno, "Correlation between structure and optical properties of Si-based alloys deposited by PECVD," *Thin Solid Films*, vol. 511-512, pp. 598–602, 2006.

[22] W. J. Soppe, H. J. Muffler, A. C. Biebericher et al., "Optical and structural properties of microcrystalline silicon, grown by microwave PECVD," in *Proceedings of the 20th European Photovoltaic Solar Energy Conference and Exhibition*, p. 10, Barcelona, Spain, June 2005.

[23] M. I. Alonso and K. Winer, "Raman spectra of c-Si1-xGex alloys," *Physical Review B*, vol. 39, no. 14, pp. 10056–10062, 1989.

[24] Y. M. Yang, X. L. Wu, G. S. Huang, D. S. Hu, and G. G. Siu, "Confinement effect of optical phonons in Si-Ge alloy nanocrystals," *Physics Letters A*, vol. 338, pp. 379–384, 2005.

[25] S. J. Yun, J. K. Kim, S. H. Lee, Y. J. Lee, and J. W. Lim, "Phase transition of hydrogenated SiGe thin films in plasma-enhanced chemical vapor deposition," *Thin Solid Films*, vol. 546, pp. 362–366, 2013.

[26] J. K. Rath, R. H. J. Franken, A. Gordijn, R. E. I. Schropp, and W. J. Goedheer, "Growth mechanism of microcrystalline silicon at high pressure conditions," *Journal of Non-Crystalline Solids*, vol. 338-340, no. 1, pp. 56–60, 2004.

[27] J. Berkowitz, G. B. Ellison, and D. Gutman, "Three methods to measure RH bond energies," *The Journal of Physical Chemistry*, vol. 98, no. 11, pp. 2744–2765, 1994.

[28] S. Hazra, A. R. Middya, S. Ray, C. Malten, and F. Finger, "Role of deposition parameters on the photovoltaic quality of amorphous silicon germanium alloys: correlation of microstructure with defect density and electronic transport," *Journal of Physics D: Applied Physics*, vol. 34, no. 16, pp. 2475–2481, 2001.

[29] A. Morimoto, T. Miura, M. Kumeda, and T. Shimizu, "ESR and IR studies on a-$Si_{1-x}Ge_x$:H prepared by glow discharge decomposition," *Japanese Journal of Applied Physics*, vol. 20, no. 11, pp. L833–L836, 1981.

[30] W. Paul, D. K. Paul, B. von Roedern, J. Blake, and S. Oguz, "Preferential attachment of H in amorphous hydrogenated binary semiconductors and consequent inferior reduction of pseudogap state density," *Physical Review Letters*, vol. 46, no. 15, pp. 1016–1020, 1981.

[31] C. W. Chang, T. Matsui, and M. Kondo, "Electron spin resonance study of hydrogenated microcrystalline silicon-germanium alloy thin films," *Journal of Non-Crystalline Solids*, vol. 354, no. 19-25, pp. 2365–2368, 2008.

[32] M. Kondo, M. Fukawa, L. Guo, and A. Matsuda, "High rate growth of microcrystalline silicon at low temperatures," *Journal of Non-Crystalline Solids*, vol. 266–269, pp. 84–89, 2000.

[33] O. Vetterl, F. Finger, R. Carius et al., "Intrinsic microcrystalline silicon: a new material for photovoltaics," *Solar Energy Materials and Solar Cells*, vol. 62, no. 1, pp. 97–108, 2000.

[34] V. A. Burrows, Y. J. Chabal, G. S. Higashi, K. Raghavachari, and S. B. Christman, "Infrared spectroscopy of Si(111) surfaces after HF treatment: hydrogen termination and surface morphology," *Applied Physics Letters*, vol. 53, no. 11, pp. 998–1000, 1988.

[35] A. C. Bronneberg, A. H. M. Smets, M. Creatore, and M. C. M. van de Sanden, "On the oxidation mechanism of microcrystalline silicon thin films studied by Fourier transform infrared spectroscopy," *Journal of Non-Crystalline Solids*, vol. 357, no. 3, pp. 884–887, 2011.

[36] A. H. M. Smets, W. M. M. Kessels, and M. C. M. van de Sanden, "Vacancies and voids in hydrogenated amorphous silicon," *Applied Physics Letters*, vol. 82, no. 10, p. 1547, 2003.

[37] M. Cardona, "Vibrational spectra of hydrogen in silicon and germanium," *Physica Status Solidi B*, vol. 118, no. 2, pp. 463–481, 1983.

[38] S. Hazra, A. R. Middya, and S. Ray, "The effect of variation in hydrogen dilution and RF power density on the properties of a-SiGe:H and related solar cells," *Journal of Physics D: Applied Physics*, vol. 29, no. 6, pp. 1666–1674, 1996.

[39] T. Brammer, H. Stiebig, A. Lambertz, W. Reetz, and H. Wagner, "Temperature dependent transport in microcrystalline PIN diodes," *Materials Research Society Symposium Proceedings*, vol. 609, article A32.3, 2000.

[40] A. H. Smets, T. Matsui, and M. Kondo, "High-rate deposition of microcrystalline silicon p-i-n solar cells in the high pressure depletion regime," *Journal of Applied Physics*, vol. 104, no. 3, Article ID 034508, 2008.

[41] T. Matsui, H. Jia, and M. Kondo, "Thin film solar cells incorporating microcrystalline $Si_{1-x}Ge_x$ as efficient infrared absorber: an application to double junction tandem solar cells," *Progress in Photovoltaics: Research and Applications*, vol. 18, no. 1, pp. 48–53, 2010.

[42] T. Fujibayashi, T. Matsui, and M. Kondo, "Improvement in quantum efficiency of thin film Si solar cells due to the suppression of optical reflectance at transparent conducting oxide/Si interface by TiO_2/ZnO antireflection coating," *Applied Physics Letters*, vol. 88, no. 18, Article ID 183508, 2006.

[43] Y. T. Huang, C. H. Hsu, and C. C. Tsai, "Enhancement of spectral response in μc-$Si_{1-x}Ge_x$:H thin-film solar cells with a-Si:H/μc-Si:H P-type window layers," *International Journal of Photoenergy*, vol. 2015, Article ID 841614, 8 pages, 2015.

[44] H. J. Hsu, S. W. Liang, Y. T. Huang, C. H. Hsu, and C. C. Tsai, "Applications of μc-SiO_x:H as integrated n-layer and back transparent conductive oxide for a-Si:H/μc-Si:H tandem cells," *Japanese Journal of Applied Physics*, vol. 53, no. 5, supplement 1, Article ID 05FV08, 2014.

[45] O. Isabella, A. H. M. Smets, and M. Zeman, "Thin-film silicon-based quadruple junction solar cells approaching 20% conversion efficiency," *Solar Energy Materials and Solar Cells*, vol. 129, pp. 82–89, 2014.